Hindawi
Geofluids
Volume 2023, Article ID 4981874, 13 pages
https://doi.org/10.1155/2023/4981874

Research Article

Study on Damage Mechanism of Waterflooding Development in Weizhou 11-4N Low-Permeability Oilfield

Yi Zhang,[1] **Pengyu Zhu**,[1] **Feng Wei**,[2] **Guoqing Xue**,[3] **Mingguang Tang**,[2] **Congdi Zhang**,[4] **and Rui Wang**[1]

[1]*Engineering Research Center of the Ministry of Education for the Development and Treatment of Low and Ultra-Low Permeability in the West of Xi'an Shiyou University, Shanxi, Xi'an 710065, China*
[2]*Zhanjiang Branch of CNOOC (China) Co., Ltd, Guangdong, Zhanjiang 524057, China*
[3]*Hainan Branch of CNOOC (China) Co., Ltd, Hainan, Haikou 570312, China*
[4]*Yakela Gas Exploitation Plant, Sinopet Northwest China Oilfield Company, Xinjiang Kuche 842017, China*

Correspondence should be addressed to Yi Zhang; zhyfly@163.com

Received 6 September 2022; Revised 11 October 2022; Accepted 15 October 2022; Published 16 February 2023

Academic Editor: Daoyi Zhu

Weizhou 11-4N oilfield is a medium-low-porosity and low-permeability reservoir. The oilfield was initially developed by edge and bottom water energy and then transferred to water injection development. Affected by poor physical properties and heterogeneity of the reservoir, the oilfield appeared in the process of water injection development. When the water injection pressure increases, the water injection volume continues to decrease, and it is difficult to meet the injection requirements. On the basis of the analysis of reservoir heterogeneity, void structure, and clay minerals of reservoir, the water injection compatibility experiment, damage evaluation experiment, and nuclear magnetic resonance-velocity sensitivity experiments were carried out to clarify the damage in the process of oilfield water flooding development. Experiments show that the main causes of damage in Weizhou 11-4N oilfield water flooding development process are water quality incompatibility and strong velocity-sensitive damage. The determination of water type shows that the injected water and formation water are $MgCl_2$ water type and $NaHCO_3$ water type, respectively, under the classification of Surin water type, resulting in the formation of scale with calcium carbonate as the main component in the reservoir. Incompatibility of water quality is an important cause of reservoir damage and scaling. In the reservoir-sensitive flow experiment, the experimental core showed strong velocity sensitivity, the average velocity sensitivity damage rate was 466.31%, and the average critical velocity was 2.98 m/d. Nuclear magnetic resonance experiments show that the core has a significant decrease in average pore size after water flooding. The main damage range is the tiny throat of 0-2 μm. In this paper, the main damage interval of velocity-sensitive damage in the Weizhou 11-4N area and the change trend of void structure after velocity-sensitive experiment are clarified by nuclear magnetic resonance and velocity sensitivity experiments. The main cause of block reservoir damage provides the basis for the oilfield to take targeted measures and provides a guarantee for the efficient development of the subsequent oilfield.

1. Introduction

Weizhou 11-4N oilfield is located in the Beibu Gulf of the South China Sea about 100 km away from Beihai city and about 50 km away from Weizhou island. It was first discovered in 1986 according to two-dimensional seismic interpretation. The Paleogene of Weizhou 11-4N Oilfield mainly develops the Weizhou formation, Liushagang formation, and Changliu formation. The main oil groups are L_1V, L_1III, and L_1I oil groups [1–5]. In the early stage of development, depletion development was adopted, then gradually adopt water injection development. In order to restore the formation energy and maintain a high oil production rate, in the process of water injection development, high injection volume water injection was used at the initial stage. After water injection development for a period of time, the water injection pressure continued to increase, and the water injection volume decreased to varying degrees.

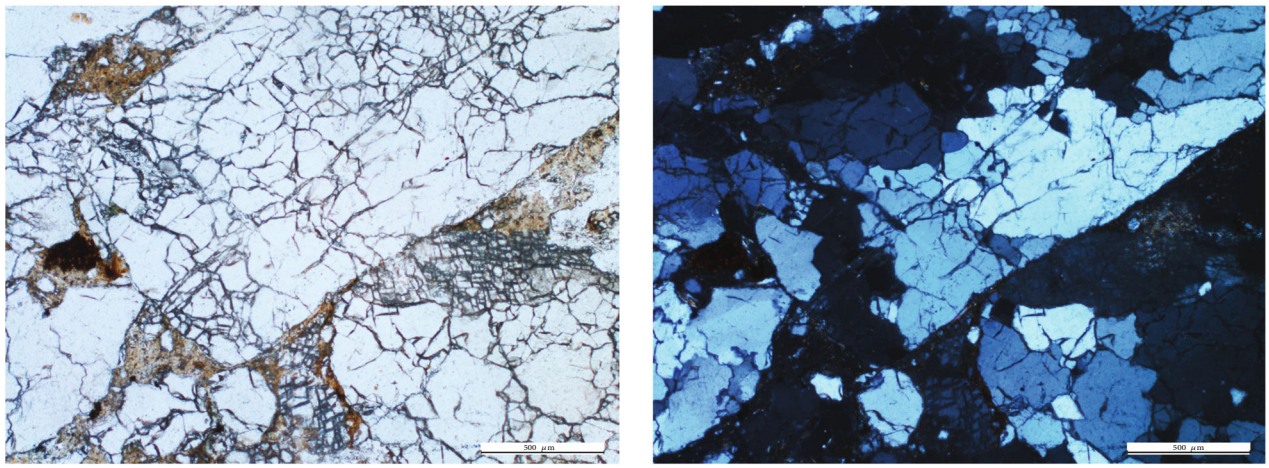

Figure 1: Thin section of core casting of L_1 section in Weizhou 11-4N oilfield.

The water injection volume of some water injection wells has been reduced by 70%, and the oil production volume of the corresponding oil production wells has also been greatly reduced compared with the initial stage of water injection, which seriously restricts the efficient development of the oil field. It is particularly important to clarify the damage to the reservoir caused by the speed sensitivity in water flooding development and to improve the development benefit for the subsequent depressurization and injection.

In 2008, Bedrikovetsky et al. [6] established a depth filter loss model through theoretical analysis and experimental research, obtained the particle concentration values at multiple points through the indoor long core segment test, and then used the least square method to obtain the core impedance model. The damage evaluation parameters of the system can be obtained. In 2009, Xijin and Feng [7] analyzed the hydration mechanism of biotite and analyzed the influence on water injection according to the hydration process. In the same year, Lijun and Yili [8] analyzed the influence of capillary self-absorption on reservoir sensitivity evaluation by using capillary self-absorption experiments on the basis of reviewing the capillary self-absorption mechanism. In 2014, on the basis of study on compatibility of water quality, Yutian et al. [9] used electron microscopy to analyze the damage characteristics of scaling after water injection, sewage reinjection, etc. and believed that water quality incompatibility and high oil content in the sewage were the main damage factor in the process of water injection.

In 2018, Ramez et al. [10] showed that low-salinity water flooding can effectively improve water flooding effect and reduce reservoir damage, and the optimal salinity is related to the physical properties of the reservoir. In the same year, Jianjun et al. [11] conducted an indoor evaluation of waterflooding and scaling, combined with the analysis of core minerals in the early and late stages of development, and clarified the reservoir scaling mechanism, and made it clear that scaling, velocity sensitivity, and water sensitivity are the main damage types. In 2019, Lei et al. [12] applied the global mobility theory to evaluate the results of water flooding experiments with different salinities and established an oil-water two-phase flow oil well productivity equation considering low-velocity non-Darcy flow and reservoir stress sensitivity. The effects of reservoir properties and oil-water two-phase seepage capacity on reservoir productivity were quantitatively evaluated. In the same year, Moghadasi et al. [13] showed that nanosilica has obvious effect of inhibiting calcium sulfate scaling in formation water with high salinity at appropriate temperature, but the effect is not obvious at low salinity.

In 2020, based on the study of reservoir geological characteristics, Dongyu et al. [14] used laboratory experiments to determine the reservoir damage mechanism during water injection and believed that strong water sensitivity and high water injection intensity were the main damages in the development process. In the same year, Wang and Zhou [15] used electron microscope scanning technology to study the difference in water plugging damage between uncracked cores and cracked cores and evaluated the improvement effect of the new nanoemulsion on microclogging and liquid flow capacity. In 2021, Zhu et al. [16] reviewed the application research progress of NMR technology in the role of polymer gels, showing that it has broad application prospects in evaluating the performance of gel and monitoring the improvement effect of gel. In 2022, Negahdari et al. [17] proposed a technology to optimize the injection water composition of low-salinity water flooding using numerical simulation. The study showed that the optimal injection water composition in the same formation is not unique. Yi et al. [18] used a neural network to predict and analyze reservoir damage based on laboratory experimental results. The above papers have done a lot of work in improving water injection effect, reducing reservoir damage and reservoir scaling mechanism, and inhibiting reservoir scaling. However, none of the above papers paid attention to the microscopic damage mechanism of the reservoir. In this paper, based on the analysis of Weizhou 11-4N reservoir characteristics, the microscopic damage mechanism of the core and the main size range of pore throat damage will be studied. The potential damage mechanism of the reservoir was analyzed by scanning electron microscope, X-ray diffraction, and other experimental results, and the damage mechanism of the reservoir was clarified by the indoor flooding

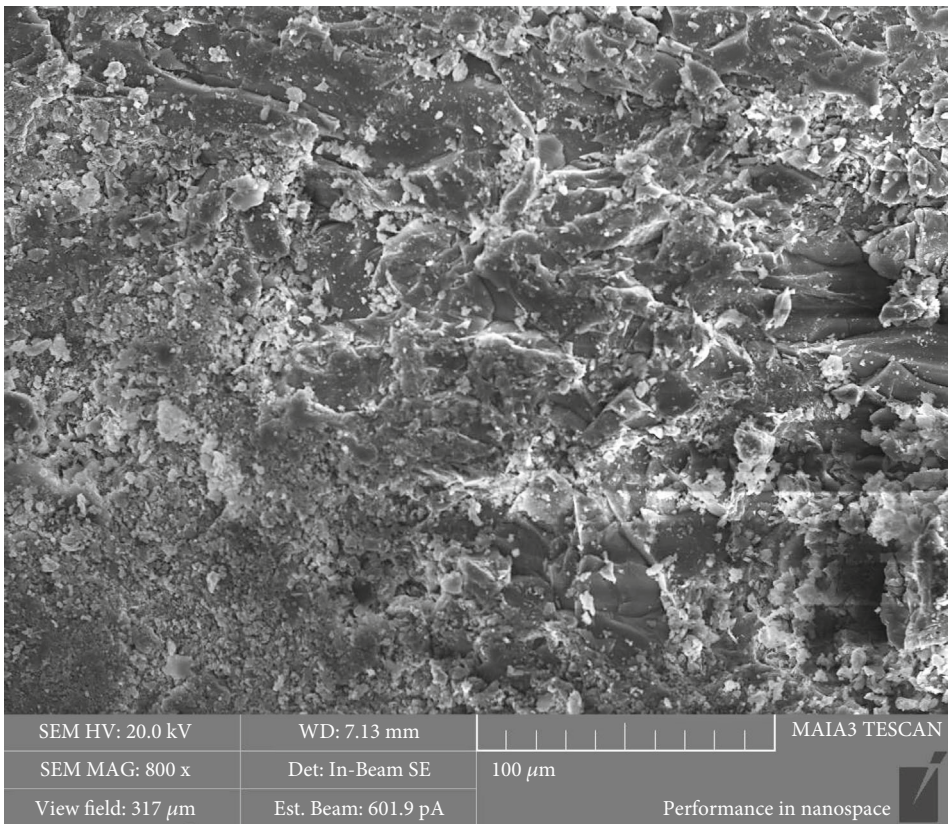

(a) A5 core Panorama

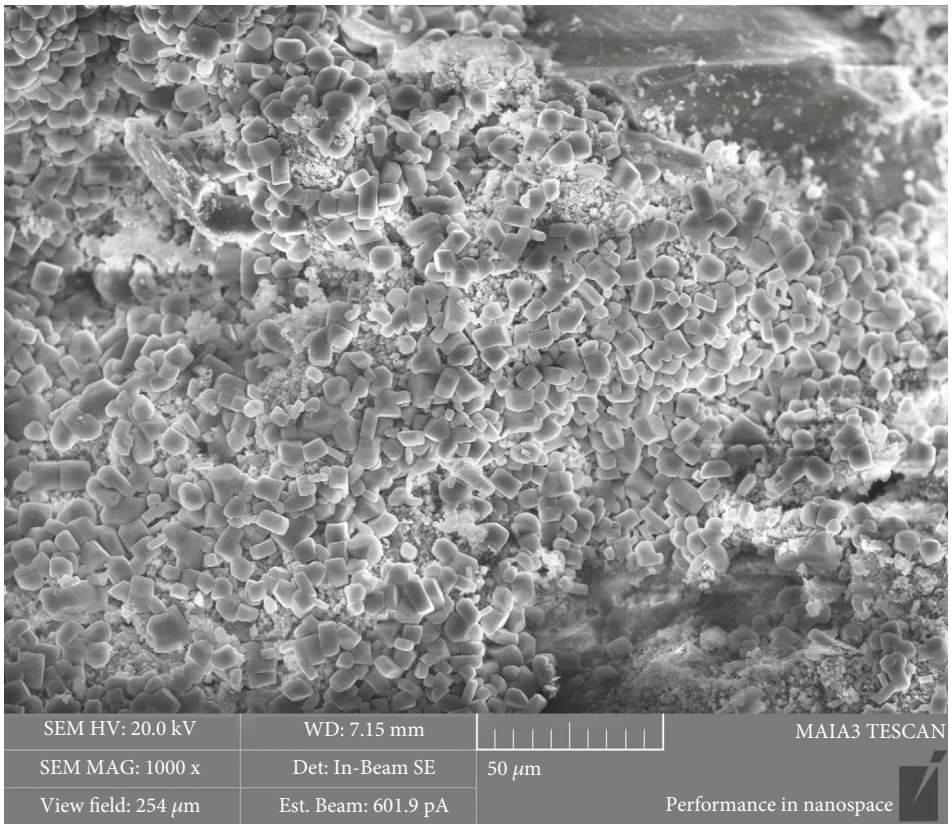

(b) A5 Core magnification (1000 times)

Figure 2: Continued.

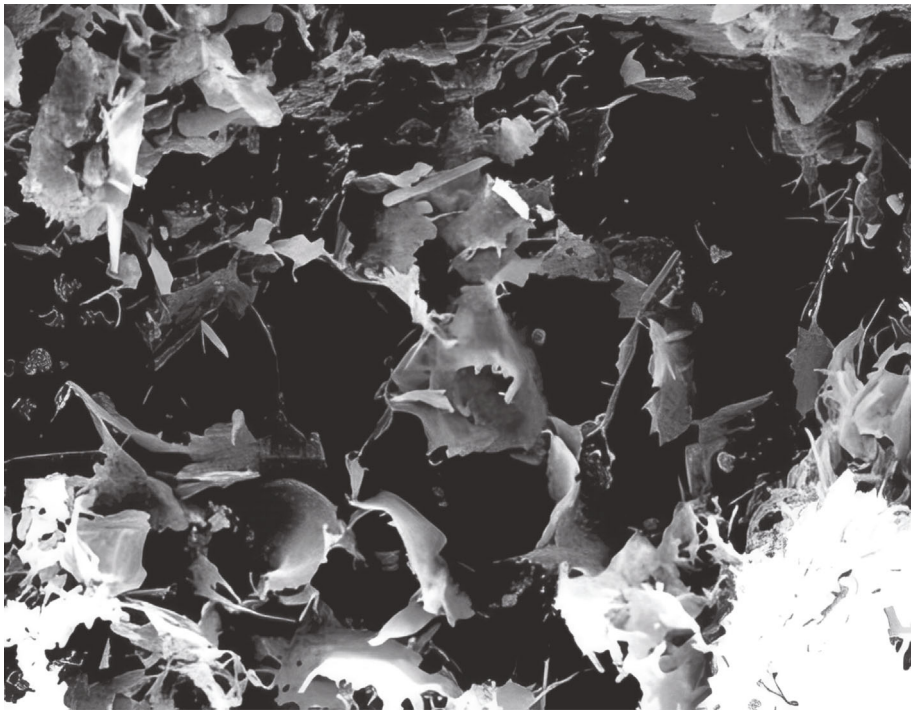

(c) Intergranular honeycomb layer

(d) Intergranular flaky illite

Figure 2: Core electron microscopic diagram of Liu 1 formation in Weizhou 11-4N oilfield (Wang Yanxing, [19]).

experiment. It provides strong guidance for the determination of efficient development and production and injection measures. At the same time, combined with the water quality compatibility experiment, a comprehensive analysis of the damage mechanism of water injection development in oilfields was carried out to provide reference for subsequent production practice.

2. Reservoir Overview

2.1. Analysis of Reservoir Heterogeneity. The fan delta front subfacies is developed in the L_1 section of Weizhou 11-4N, which is dominated by underwater distributary channel deposits. The lithological composition of the reservoir is relatively complex, including glutenite, coarse sandstone, and

Table 1: clay mineral composition table of L_1 section in Weizhou 11-4 N oilfield.

Number	Core number	Well depth (m)	Quartz (%)	Total amount of clay minerals (%)	Other minerals (%)	Illite (%)	Kaolinite (%)	Mixed layer of illite and montmorillonite (%)	Chlorite (%)
1	2-1	2603.09	70.50	14.40	15.10	70.00	11.00	15.00	4.00
2	2-4	2934.59	71.50	17.80	10.70	61.00	25.00	11.00	3.00
3	2-8	2217.00	85.20	8.20	6.60	44.00	32.00	18.00	6.00
4	2-10	2514.80	85.80	7.10	7.10	43.00	44.00	7.00	6.00
5	2-21	2778.00	87.50	9.10	3.40	48.00	39.00	9.00	4.00
6	2-13	3132.60	81.00	14.00	5.00	77.00	7.00	12.00	4.00
7	2-29	3139.50	83.00	15.30	1.70	68.00	11.00	14.00	7.00
8	2-35	2777.70	86.90	4.60	8.50	70.00	10.00	16.00	4.00
	Maximum value		87.50	17.80	15.10	77.00	44.00	18.00	7.00
Statistics	Maximum value		70.50	4.60	1.70	43.00	7.00	7.00	3.00
	Mean value		81.43	11.31	7.26	60.13	22.38	12.75	4.75

Table 2: Water sample ion concentration of the Weizhou 11-4N oilfield.

Water type	Cation (mg/L)			Anions (mg/L)				Total mineralization (mg/L)	pH value
	K^++Na^+	Mg^{2+}	Ca^{2+}	Cl^-	HCO_3^-	SO_4^{2-}	CO_3^{2-}		
Injection water	36.22	353.79	144.8	240.71	70.94	0.52	0	846.97	7
Formation water	2481	58	0	1427	4238	25	72	8301	7.71

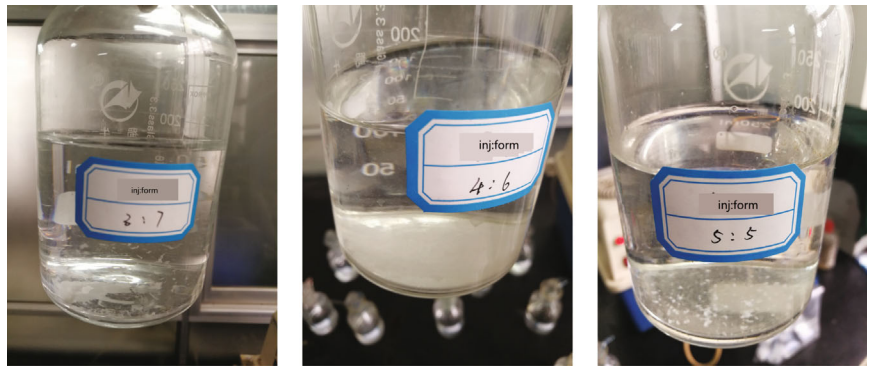

Figure 3: Some samples with serious scale after 140 days of standing.

silt-fine sandstone. The lithology is mixed and the sorting ability is poor; the overall reservoir distribution is not stable, and the vertical interlayers are developed, which are thin and interbedded, the plane phase change is fast, the lateral change is violent, and the heterogeneity is strong [5, 19]. The relative physical properties of several cores obtained from the field were measured, and the porosity of the cores was mainly distributed in the range of 9.65% to 22.27%, with an average of 15.37%; the average permeability of the cores was 12.62×10^{-3} μm^2.

2.2. Analysis of Pore Structure. Through the analysis of core pore throat by casting thin section (Figure 1), there are very few carbonate dissolved pores and intercrystalline pores in the core, and the feldspar dissolved pores are formed by local dissolution of feldspar. The quartz is cut through by microfractures and filled with micrite calcite. The intercrystalline pores and dissolved pores are randomly distributed, and the connectivity is general, but the heterogeneity is strong.

It can be seen from the core electron microscope images (Figures 2(a) and 2(b)) that the core pores are poorly developed, mainly intercrystalline pores, accompanied by a certain amount of feldspar dissolved pores, and there are few intercrystalline dissolved pores [5, 20]. The diagenetic authigenic clay mixed layer and chlorite were produced in a liner type and filled with pores, and no increase in quartz was evident. Combined with the research of Yanxing et al. (Figures 2(c) and 2(d)), the dissolution pores on the grain surface in this area were observed. There are mixed layers of authigenic quartz, flaky illite, and lamellar illite. During waterflooding development, illite can migrate under the action of water and fluid to block the pore throat, which

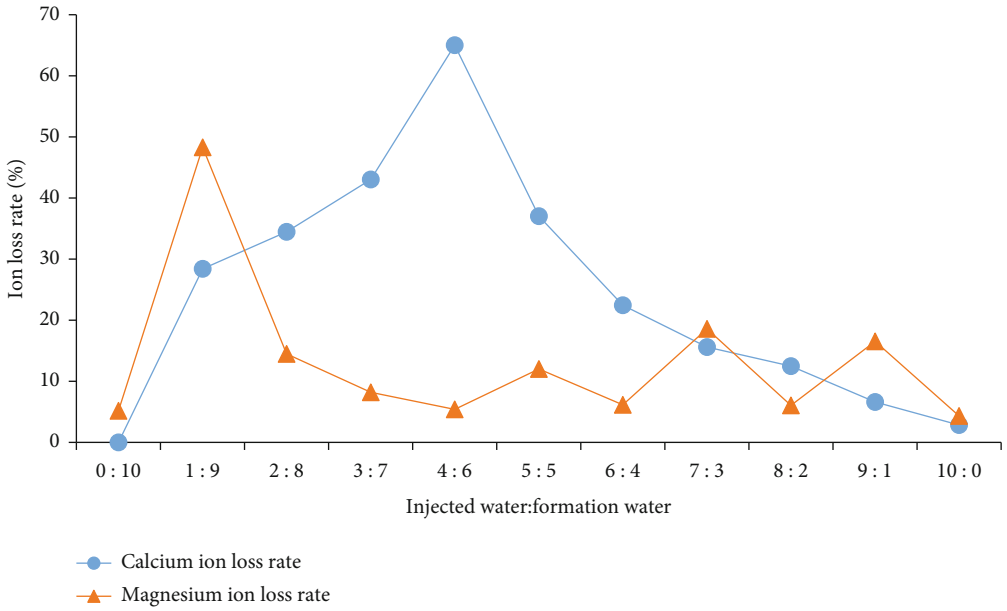

Figure 4: Water quality compatibility data chart.

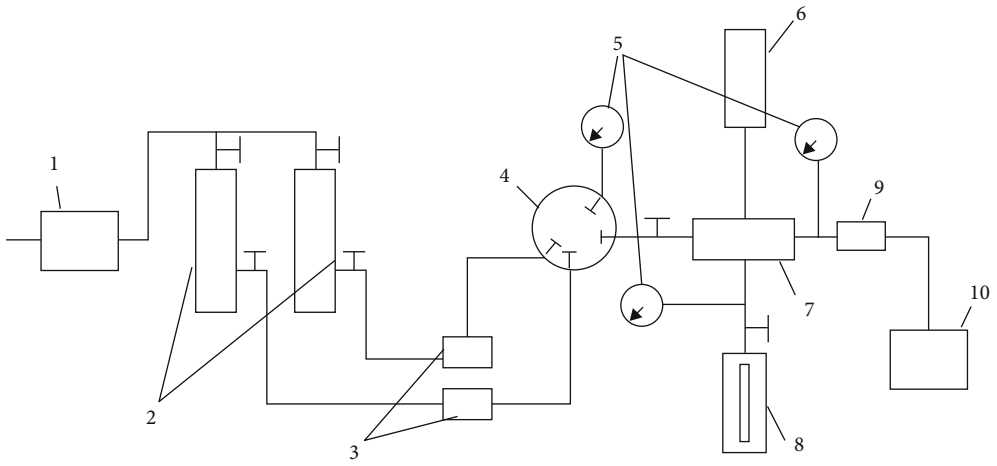

1-High pressure micro flow displacement advection pump
2-Sealed middle container
3-Filter
4-Six-way valve
5-Pressure gauge
6-Thermostat
7-Core holder
8-Manual confining pressure pump
9-Back pressure valve
10-Water separator

Figure 5: Flow chart of sensitivity experiment. 1: high pressure microflow displacement advection pump; 2: sealed middle container; 3: filter; 4: six-way valve; 5: pressure gauge; 6: thermostat; 7: core holder; 8: manual confining pressure pump; 9: back pressure valve; 10: water separator.

has potential risk of speed-sensitive and water-sensitive damage, which carries particles through fluid flushing and leads to reservoir plugging.

2.3. Reservoir Clay Mineral Analysis. The analysis of clay minerals in the cores by X-ray diffraction (Table 1) shows the content of clay minerals in the L_1 section is 4.6%-17.8%, with an average of 11.31%. Among the clay minerals, the content of illite, which is easy to cause water-sensitive and speed-sensitive damage, is relatively high, followed by kaolinite. The honeycomb-like and flake-like microscopic morphology of illite and kaolinite determines that when the injected fluid flow rate and salinity change, the particles may disperse and migrate, which in turn blocks other pore throats, resulting in a decrease in permeability and a decrease in the ability to absorb and inject water. In the L_1

Table 3: Experimental results of velocity sensitivity, water sensitivity and salt sensitivity in the Weizhou 11-4N oilfield.

Type of experiment	Sample number	Well depth (m)	Lithology	Damage rate (%)	Damage assessment
Speed sensitivity	A1	2208.53	Sandstones	96.68	Strong
Speed sensitivity	A2	2209.17	Sandstones	1455.77	Strong
Speed sensitivity	A3	2086.76	Sandstones	133.36	Strong
Speed sensitivity	A4	2171.89	Sandstones	39.05	Moderately weak
Water sensitivity	B1	2087.67	Sandstones	36.6	Moderately weak
Water sensitivity	B2	2086.79	Sandstones	78.89	Strong
Water sensitivity	B3	2209.41	Sandstones	33.04	Moderately weak
Water sensitivity	B4	2092.31	Sandstones	32.79	Moderately weak
Water sensitivity	B5	2088.73	Sandstones	41.27	Moderately weak
Water sensitivity	B6	2087.49	Sandstones	29.75	Weak
Water sensitivity	B7	2209.58	Sandstones	13.51	Weak
Salt sensitivity	C1	2209.04	Sandstones	89.11	Strong
Salt sensitivity	C2	2230.7	Sandstones	48.92	Moderately weak
Salt sensitivity	C3	2221.84	Sandstones	/	None
Salt sensitivity	C4	2225.38	Sandstones	35.35	Moderately weak

section, illite accounts for 60.13% of clay minerals on average, kaolinite accounts for 22.38% on average, and velocity-sensitive clay minerals account for as high as 82.51%. There is a potential risk of relatively strong velocity-sensitive damage in the reservoirs of L_1 section.

3. Compatibility Test of Injected Water

On the basis of the ion composition of formation water obtained from the analysis of oilfield data, the sampling was measured according to "SL394.1-2007 Determination of 34 Elements such as Lead, Cadmium, Vanadium, Phosphorus - Inductively Coupled Plasma Atomic Emission Spectroscopy (ICP-AES)." The cations of the injected water were then measured by the EDTD volumetric method, the acid-base titration method, and the silver nitrate method to measure the sulfate ion content, the carbonate, bicarbonate ion concentration, and the chloride ion concentration. The measurement results are shown in Table 2. According to the difference in water type and salinity between the injected water and the formation water from external operations, the injected water and formation water were analyzed by the Surin water type classification. The experimental results show that the formation water type is $NaHCO_3$, while the injection water type is $MgCl_2$. According to the difference in ion and salinity of formation water and injection water, there is a potential incompatibility problem [21–27].

To clarify the compatibility of injected water and formation water, an appropriate amount of simulated formation water and injection water were prepared according to the analysis results of oilfield water samples. On the basis of filtering membrane to remove suspended particles, the injected water and formation water were fully mixed according to the following proportions 1 : 0, 9 : 1, 8 : 2, 7 : 3, 6 : 4, 5 : 5, 4 : 6, 3 : 7, 2 : 8, 1 : 9, and 0 : 1 and then 11 groups of it were made. After mixing, take 200 mL of each water sample and place it in a closed sampling bottle and stand at 26°C for 140 days to observe the compatibility of injected water and formation water under different mixed concentrations. We filter on the filter and analyze its ion concentration. The results of naked eye observation and the change of ion concentration of water samples are shown in Figures 3 and 4, respectively. It can be seen from Figure 3 that the injection water and formation water have obvious scaling at 2 : 8-5 : 5, that is, the mixed water of 20% to 50% of the injection water. Furthermore, according to the change diagram of mixed water ion concentration (Figure 4), it can be seen that the mixed water samples with a calcium ion loss rate of more than 30% have scaling phenomenon, and magnesium ions have little change. The results show that the injection water and formation water in this area scale were changed. The sample is mainly calcium carbonate. The laboratory evaluation experiment on the compatibility of injected water and formation water shows that Weizhou 11-4N oilfield has a certain water quality incompatibility problem. During long-term water injection development, due to the influence of calcium carbonate scaling at some mixed concentrations, the pore throats in the formation may be blocked. As a result, the formation permeability decreases, and the water injection volume decreases and the water injection pressure increases.

Table 4: Evaluation index of damage rate.

Damage rate (%)	Degree of damage
Dv ≤ 5	None
$5 < D_v \leq 30$	Weak
$30 < D_v \leq 50$	Moderately weak
$50 < D_v \leq 70$	Moderately strong
$D_v > 70$	Strong

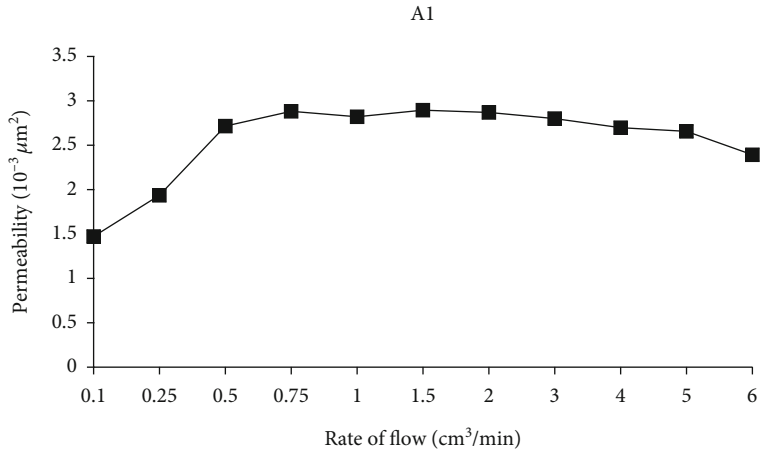

(a) A1

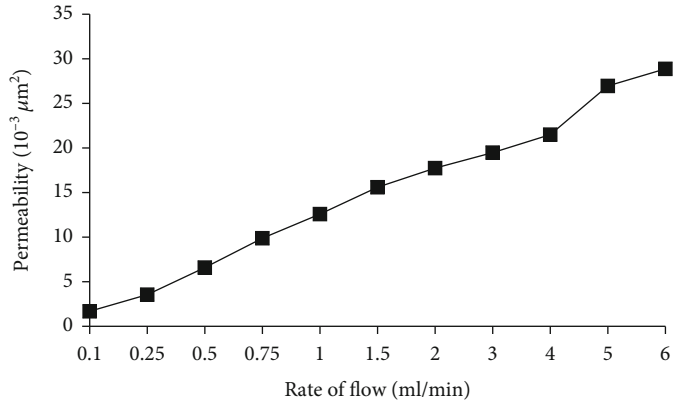

(b) A2

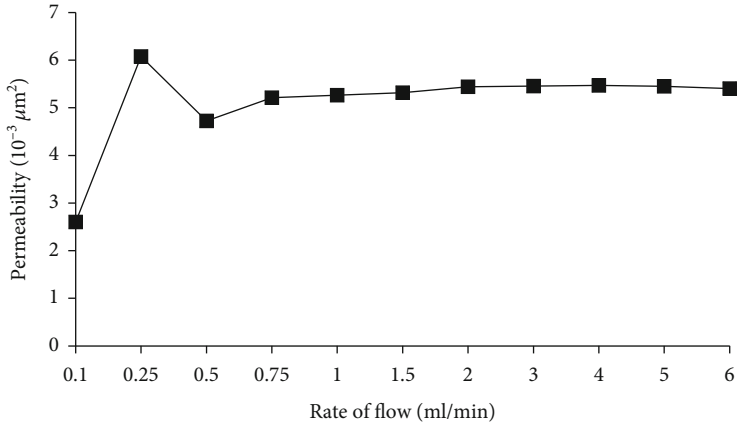

(c) A3

Figure 6: Continued.

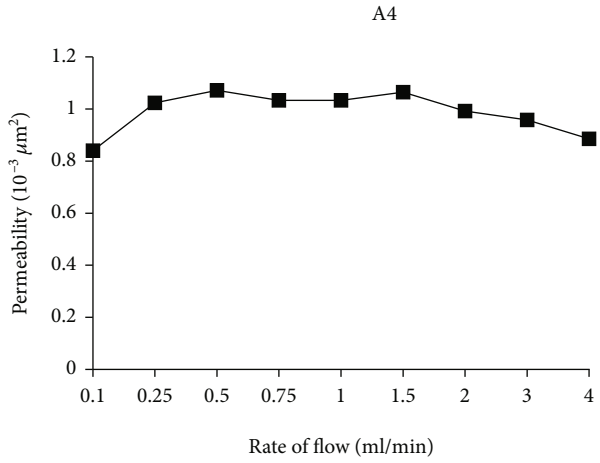

(d) A4

Figure 6: The relationship between reservoir flow rate and permeability.

4. Damage Evaluation Experiment

4.1. Preparation and Process of the Experiment. Firstly, according to "GB/T 29172-2012 Core Analysis Method," the experimental core was prepared, the porosity and permeability were measured by gas, and the simulated formation water was saturated by vacuum pumping. Then, the reservoir sensitivity experiment of Weizhou 11-4N oilfield was carried out according to the procedures and evaluation indicators specified in the petroleum industry standard "SY/T 5358-2010 Evaluation Method of Reservoir Sensitivity Flow Experiment." The experimental process is shown in Figure 5, which mainly includes high-pressure microflow displacement advection pump, manual confining pressure pump, sealed intermediate container, core holder, pressure gauge, and flow meter.

4.2. Result Analysis. According to the experimental method and standard of "SY/T 5358-2010 Experimental Evaluation Method for Reservoir Sensitive Flow," laboratory evaluation experiments on velocity-sensitive, water-sensitive, and salt-sensitive damage of 15 cores in the Weizhou 11-4N oilfield were carried out, respectively. The data and experimental evaluation results are shown in Table 3. According to the damage rate evaluation index (Table 4), it can be seen that the Weizhou 11-4N oilfield has velocity sensitivity ranging from moderately weak to strong, of which the strong velocity sensitivity accounts for 75%. There are water sensitivities ranging from weak to strong, with moderately weak water sensitivities prevailing. There are salt sensitivities ranging from non-existent to strong, with moderately weak salt sensitivities prevailing. At the same time, combined with the previous experimental results, there are alkali-sensitive and acid-sensitive damages from no to weak.

From the experimental results of velocity-sensitive damage evaluation of several cores (Figure 6), it can be seen that except for the A2 core, whose permeability increases with the increase of injection rate, the other three cores all show that the permeability first increases and then decreases with the increase of injection rate. According to the formula $D_v = ((|K_n - K_i|)/K_i) \times 100\%$, the core permeability transformation rate caused by velocity sensitivity is calculated, where K_n is the permeability of the rock sample under different flow rates, and K_i is the permeability under the minimum flow rate; the calculation formula of the damage rate is $D_V = \max(D_{v2}, D_{v3}, \cdots, D_{vn})$, the velocity-sensitive damage rate of the 4 cores is 27.56%~1607.62%, with an average of 466.31%, and the critical flow rate is 2.68~3.48 m/d, with an average of 2.98 m/d.

Further analysis of the results of the velocity sensitivity experiments on the four cores shows that, except for the A2 core, the other three cores all show that the permeability becomes an inflection point before and after the injection flow rate of 0.75 cm^3/min. When the injection flow rate is less than 0.75 cm^3/min, it increases with the injection rate. The permeability of the core increases, and the permeability decreases with the increase of the flow rate after the injection flow rate is greater than 0.75 cm^3/min. By analyzing the relationship between different flow rates and permeability damage rate (Figure 7), at low flow rate (flow rate less than 0.75 cm^3/min), the permeability increases with the increase of flow rate, and the permeability damage rate increases with the increase of flow rate and increase. At high flow rate (flow rate greater than 0.75 cm^3/min), the permeability decreases with the increase of flow rate, and the permeability damage rate also decreases with the increase of flow rate. Combined with the analysis of mineral composition and clay minerals, it is believed that when the seepage velocity is low, the migration of loose small particles in the core increases the storage space and improves the core permeability. Poor rock particles begin to migrate, migrate deep into the formation, and plug at deep pore throats, resulting in a decrease in overall permeability. It is reflected in the mine field that the water absorption capacity is reduced

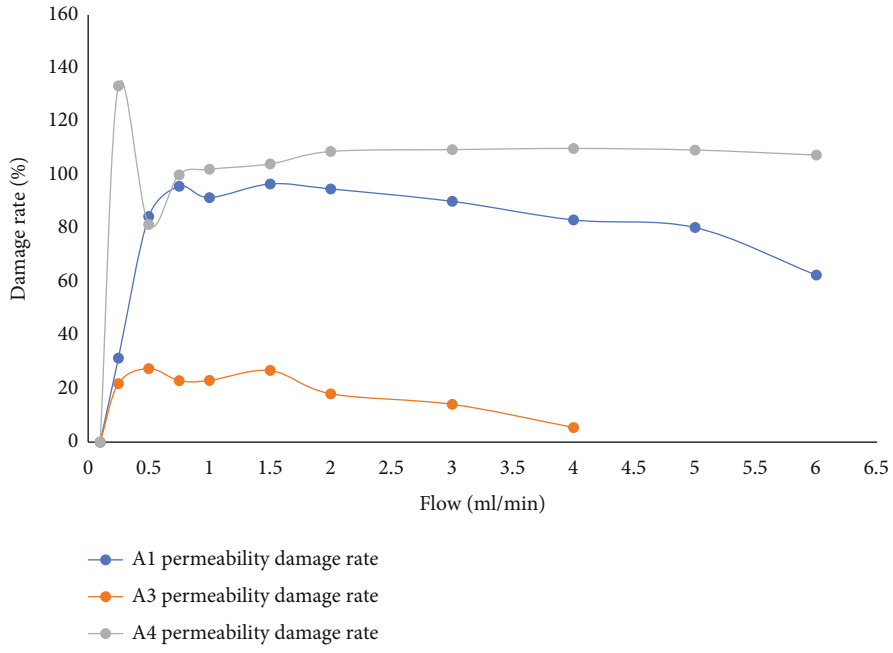

Figure 7: Relationship between damage degree of core permeability and flow rate.

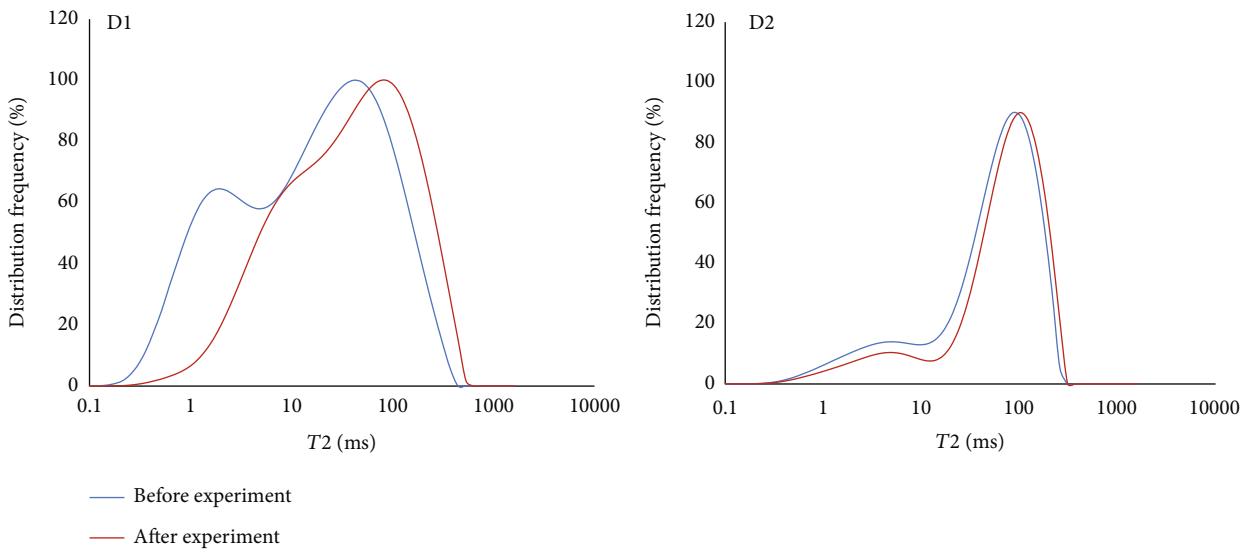

Figure 8: Contrast figure of nuclear magnetic resonance curves before and after core velocity-sensitive experiment.

and the water injection pressure is increased. Due to the short length of the core used in the experiment, the phenomenon of particle migration blocking the pore throat is not obvious enough, and the decrease of permeability is small. After analyzing the experimental process, it is believed that the A2 core has serious internal fractures due to external force factors before the experiment, which leads to the continuous increase of permeability.

In order to verify the blockage caused by the velocity-sensitive experiment, two cores D1 and D2 were selected for velocity-sensitive experiments according to the above standards, and then, the two cores before and after displacement were tested by nuclear magnetic resonance. Comparing the NMR data before and after displacement, it can be observed that after the velocity sensitivity test, the distribution frequency curves of the two cores have decreased to varying degrees in the interval of 0.1-100 ms. It shows that the proportion of small voids and small pore throats in the cores of the two samples decreased to varying degrees after the test. Larger pores and pore throats rise slightly or remain basically unchanged.

According to the data obtained by the constant-rate mercury intrusion experiment on the D1 and D2 cores before and after the experiment, the distribution map of

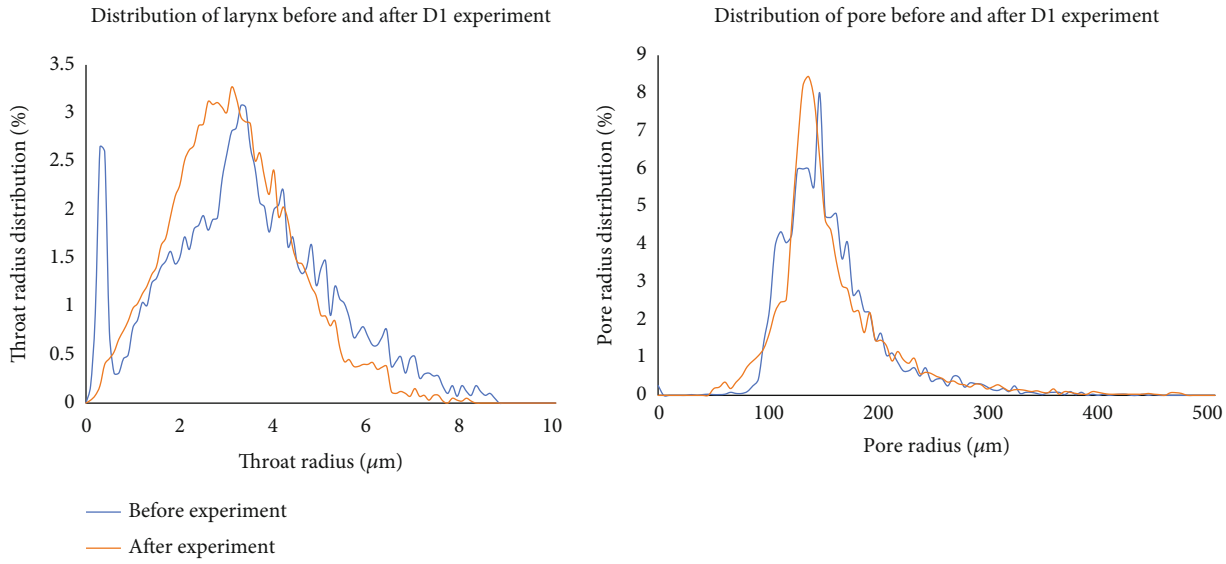

Figure 9: D1 distribution of pore and throat before and after core experiment.

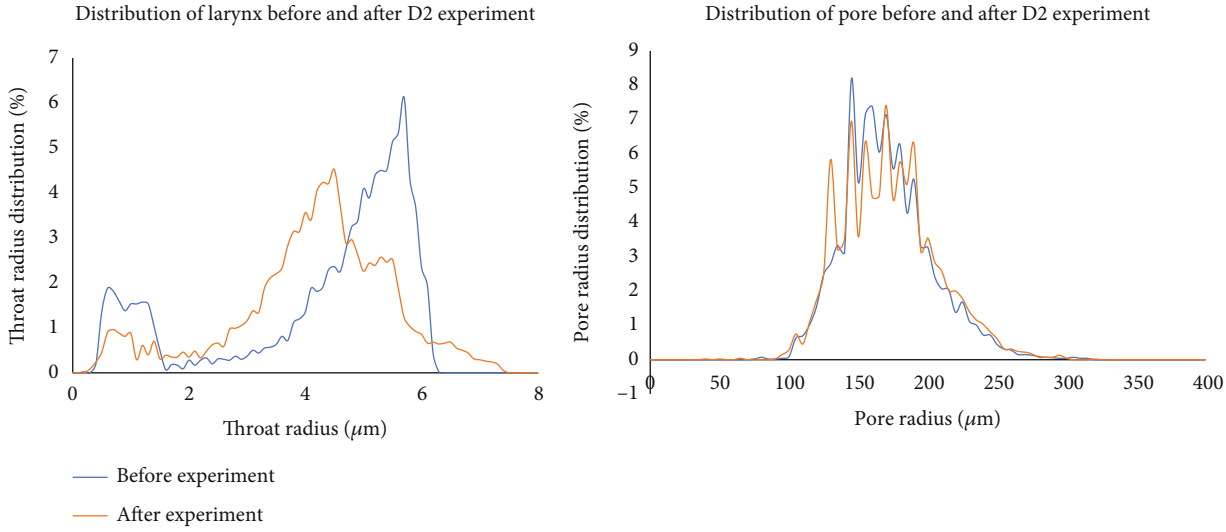

Figure 10: D2 distribution of pore and throat before and after core experiment.

the pores and throats before and after the D1 and D2 cores are drawn. From the analysis of Figures 8–10, it can be seen that after the velocity sensitivity test of the two cores D1 and D2, the proportion of pores with a size of 0-2 μm has decreased significantly. The proportion of larger pores (2-5 μm) increased slightly or remained basically unchanged. D2 showed a significant decrease in the pore throat ratio in the range of 5-6 μm. The pores with larger size were not significantly affected, and the overall proportion of the pores basically did not change before and after the experiment. Based on the analysis of the previous experiments, it is believed that in the velocity-sensitive experiment, when the flow velocity exceeds a certain limit, the loose small particles on the walls of the larger pore throats in the core begin to peel off, and these small particles migrate with the fluid. When the channel is blocked, the roars with a size of 0-2 μm decrease significantly after the test, while the proportion of the throats with larger size increases slightly due to particle migration. The decrease in the proportion of pore throats in the 5-6 μm range of the D2 core is presumed to be caused by operational errors or external factors during the experiment.

At the same time, according to the data measured in the experiment, the main flow throat radius of the D1 core is 3.42 μm before the experiment and 2.97 μm after the experiment. The average throat radius was 3.84 μm before the experiment and 3.41 μm after the experiment (Table 5). The radius of the mainstream throat was 4.68 μm before the D2 core experiment and 3.98 μm after the experiment. The average throat radius was 4.63 μm before the experiment and 4.36 μm after the experiment (Table 6).

Table 5: Throat data before and after the D1 core experiment.

	Mainstream throat radius (μm)	Maximum throat radius (μm)	Average throat radius (μm)	Relative sorting coefficient	Homogeneity coefficient
Before speed sensitivity experiment	3.42	8.70	3.84	0.47	0.39
After speed sensitivity experiment	2.97	8.20	3.41	0.40	0.38

Table 6: Throat data before and after the D2 core experiment.

	Mainstream throat radius (μm)	Maximum throat radius (μm)	Average throat radius (μm)	Relative sorting coefficient	Homogeneity coefficient
Before speed sensitivity experiment	4.68	6.30	4.63	0.37	0.69
After speed sensitivity experiment	3.98	7.40	4.36	0.32	0.56

5. Conclusion

(1) The content of clay minerals that are easy to cause velocity-sensitive damage in the first-stage reservoir of the Weizhou 11-4N oilfield exceeds 80%, and other nonclay mineral formation particles such as calcite and anorthite will also migrate with the fluid. Effects of potential sensitivity damage

(2) According to the reservoir compatibility experiment, the formation water and injection water of the Weizhou 11-4N oilfield are $NaHCO_3$ water type and $MgCl_2$ water type, respectively, and there is water quality incompatibility. It is easy to form calcium carbonate precipitation, which blocks the pore throat and causes the permeability to decrease

(3) The velocity sensitivity test results show that the reservoir in the first stage of the flow is strongly velocity-sensitive damage, with an average damage rate of 466.31% and an average critical flow rate of 2.98 m/d. Add clay stabilizers and other methods to reduce reservoir damage

(4) NMR experiments show that the velocity-sensitive damage in Weizhou 11-4 N oilfield mainly occurs in the tiny throat of 0-2 μm, and the main damage is caused by the blockage of the throat caused by particle migration. Velocity-sensitive lesions in larger throats and pores were less pronounced. After the test, the average throat radius of the two cores decreased. It can be concluded that the main reason for velocity sensitivity in the Weizhou 11-4N oilfield is the blockage of tiny throats caused by particle migration

(5) Long-term water flooding development under the action of various factors such as scaling and velocity sensitivity, the pore size of the reservoir tends to decrease, which will lead to a decrease in its permeability, and a decrease in water absorption capacity, which makes water flooding difficult

Data Availability

The (data type) data used to support the findings of this study are available from the corresponding author upon request.

Conflicts of Interest

The authors declare that they have no competing of interest.

Acknowledgments

This work is financially supported by the Development Department of Zhanjiang Branch of China National Offshore Oil Corporation (CNOOC) (China) and Key Research and Development Program of Shaanxi (Program No. 2023-YBGY-316).

References

[1] Y. Weixuan, "Nanhai West oil company will develop wei11-4 oilfield for the first time," *Petroleum Exploration and Development*, no. 6, p. 88, 1988.

[2] F. Dianjing, "Logging evaluation method and application of reservoir sensitivity in Weizhou 11-1n oilfield," *Inner Mongolia Petrochemical Industry*, vol. 37, no. 1, pp. 115–118, 2011.

[3] J. Ping, Z. Hui, W. Wenjuan, L. Biao, and T. Mingguang, "Efficient development strategy of low permeability complex fault block reservoir in Liushagang Formation of Weizhou 11-4n oilfield," *China Offshore Oil and Gas*, vol. 30, no. 6, pp. 86–91, 2018.

[4] W. Feng, L. Yuelin, and M. Guangchun, "Reservoir configuration modeling of fan delta in the first member of Liushagang Formation of Weizhou 11-1n oilfield in the western South China Sea," *China Offshore Oil and Gas*, vol. 31, no. 2, pp. 93–102, 2019.

[5] L. Shiju, G. Gang, X. Xinde et al., "Source control characteristics of oil and gas migration and accumulation in Weizhou 11-4-weizhou 11-4n oilfield, Weixinan Sag, Beibu Gulf Basin," *Natural Gas Geoscience*, vol. 30, no. 9, pp. 1312–1318, 2019.

[6] P. G. Bedrikovetsky, A. S. Vaz, C. J. Furtado, and A. L. de Souza, "Formation damage evaluation from non-linear skin growth during coreflooding," in *Paper presented at the SPE International Symposium and Exhibition on Formation Damage Control*, Lafayette, Louisiana, USA, 2008.

[7] X. Xijin and Z. Feng, "Biotite hydration mechanism and its impact on water injection development," *Journal of Southwest Petroleum University (Science & Technology Edition)*, vol. 31, no. 2, pp. 81–184, 2009.

[8] Y. Lijun and K. Yili, "Research progress on capillary self absorption of oil and gas reservoir rocks," *Journal of Southwest Petroleum University (Science & Technology Edition)*, vol. 31, no. 4, pp. 112–116, 2009.

[9] F. Yutian, T. Hongming, L. Shu, W. Yanling, and C. Chao, "Analysis of reservoir damage mechanism during water injection in Bozhong 28-2nan oilfield," *Oilfield Chemistry*, vol. 31, no. 3, pp. 371–399, 2014.

[10] R. A. Nasralla, H. Mahani, H. A. van der Linde et al., "Low salinity waterflooding for a carbonate reservoir: experimental evaluation and numerical interpretation," *Journal of Petroleum Science and Engineering*, vol. 164, pp. 640–654, 2018.

[11] S. Jianjun, T. Hongming, W. Yijun, G. Xiaoping, and Y. Hao, "Study on reservoir scaling mechanism of Shahejie Formation in Qikou 18-1 oilfield and its impact on water injection development," *Oil and Gas Reservoir Evaluation and Development*, vol. 8, no. 3, pp. 40–45, 2018.

[12] L. Wang, H. Zhang, X. Peng et al., "Water-sensitive damage mechanism and the injection water source optimization of low permeability sandy conglomerate reservoirs," *Petroleum Exploration and Development*, vol. 46, no. 6, pp. 1218–1230, 2019.

[13] R. Moghadasi, A. Rostami, A. Tatar, and A. Hemmati-Sarapardeh, "An experimental study of nanosilica application in reducing calcium sulfate scale at high temperatures during high and low salinity water injection," *Journal of Petroleum Science and Engineering*, vol. 179, pp. 7–18, 2019.

[14] P. Dongyu, T. Hongming, S. Jincheng, Z. Ju, and Z. Feng, "Study on damage mechanism during water injection in pl19-9 oilfield," *Discussion on Geological Prospecting*, vol. 35, no. 2, pp. 187–196, 2020.

[15] J. Wang and F. Zhou, "Cause analysis and solutions of water blocking damage in cracked/non-cracked tight sandstone gas reservoirs," *Petroleum Science*, vol. 18, pp. 219–233, 2021.

[16] D. Y. Zhu, Z. H. Deng, and S. W. Chen, "A review of nuclear magnetic resonance (NMR) technology applied in the characterization of polymer gels for petroleum reservoir conformance control," *Petroleum Science*, vol. 18, no. 6, pp. 1760–1775, 2021.

[17] Z. Negahdari, S. Khandoozi, M. Mojtaba Ghaedi, and R. Malayeri, "Optimization of injection water composition during low salinity water flooding in carbonate rocks: a numerical simulation study," *Journal of Petroleum Science and Engineering*, vol. 209, article 109847, 2022.

[18] Z. Yi, Z. Ningsheng, L. Xiangfang, L. Hua, and Y. Juan, "Rapid prediction of reservoir sensitivity using neural network information fusion technology," *Drilling and Production Technology*, vol. 29, no. 3, pp. 50–125, 2006.

[19] W. Yanxing, *Study on sensitivity evaluation and protection measures under reservoir conditions in Weizhou 11-4n oilfield*, Changjiang University, 2015.

[20] H. Yaotu, P. Mingyue, W. Xiaopeng, and L. Jiayu, "Protection technology of unconsolidated sandstone complex pressure reservoir," *Daqing Petroleum Geology and Development*, vol. 36, no. 5, pp. 124–130, 2017.

[21] Z. Congdi, *Analysis on influencing factors of water injection in Weizhou low permeability reservoir and research on injection increasing measures*, Xi'an Shi You University, 2021.

[22] P. Mohammadalinejad, N. Hosseinpour, N. Rahmati, and M. R. Rasaei, "Formation damage during oil displacement by aqueous S_iO_2 nanofluids in water-wet/oil-wet glass micromodel porous media," *Journal of Petroleum Science and Engineering*, vol. 182, article 106297, 2019.

[23] Z. Wang, Y. Zhang, and H. Liao, "Experimental investigation on precipitation damage during water alternating flue gas injection," *Oil & Gas Science and Technology-Revue D IFP Energies Nouvelles*, vol. 75, p. 45, 2020.

[24] J. Z. Wang, X. K. Song, L. T. Sun, Y. C. Fu, and J. J. Xu, "Water quality sensitivity and characterization of permeability of waterflooding sandstone reservoirs," *Petroleum Science and Technology*, vol. 39, no. 3, pp. 88–100, 2021.

[25] Z. Zhichao, L. Daiqiang, X. Hongrong, H. Fengze, X. Rui, and L. Yuhang, "Measures of formation damage and protection in the water-injection process —the A block in Xinjiang oil filed," *IOP Conference Series: Earth and Environmental Science*, vol. 651, no. 3, article 032042, 2021.

[26] Q. Sajjad, G. Abdolah, A. Amin, M. Santos Rafael, S. M. Saeid, and N. Milad, "Experimental and modelling approach to investigate the mechanisms of formation damage due to calcium carbonate precipitation in carbonate reservoirs," *Journal of Petroleum Science and Engineering*, vol. 205, article 108801, 2021.

[27] Y. Zhang, B. Zhang, Y. Yang, B. Liu, and L. Shen, "Storage ratio of CO_2 miscible flooding in Chang 8 reservoir of H block in Ordos Basin under different injection methods," *Frontiers in Energy Research*, vol. 10, article 848324, 2022.